8umerical investigation on cooling performance of phase change assisted direct ventilation system for data center

Lingyan Yang[a], Zujing Zhang[a*], Jiri Zhou[b], Ruiyong Mao[a], Hongwei Wu[c], Xing Liang[d]

[a] College of Civil Engineering, Guizhou Provincial Key Laboratory of Rock and Soil Mechanics and Engineering Safety, State Key Laboratory of Public Big Data, Guizhou University, Guiyang 550025, China

[b] China MCC5 Group CORP.LTD., MCC5 Tower, No. 9 Wuye Road, Jinjiang District, Chengdu, 610000, China

[c] School of Physic, Engineering and computer science, University of Hertfordshire, Hatfield, AL10 9AB, United Kingdom.

[d] School of Computer Science and Mathematics, Kingston University London, KT1 2EE, United Kingdom

[*]Corresponding author: tel: +86 185 2391 9513 email: zjzhang3@gzu.edu.cn.

Abstract: Traditional data centers often use mechanical cooling systems, leading to high energy consumption and waste of natural cooling resources. Thus, a novel phase change ventilation device that combines natural cooling with phase change storage has been designed to maintain continuous natural cooling of the data center by storing cold energy from the natural cold air using phase change plates (PCPs), and eliminate the reliance on mechanical refrigeration in traditional data centers and achieving energy savings. In this study, the cooling performance of the proposed device is numerically analyzed and the feasibility of the model is verified by experiments, filling the research gap in data centers for this method. Considering main effectors, i.e., the inlet air velocity (IAV), inlet air temperature (IAT), phase change plate thickness (PCPT), phase change temperature (PCT), and thermal conductivity of encapsulation material (TCEM) on the cooling performance of the device. The results show that: (1) Phase change ventilation device can reduce the IAT of 34°C by an average of 2.53 °C within 8 hours. (2) When the IAV increases from 1 m/s to 4 m/s, the average cooling performance of the phase change ventilation device decreases by 62.93%. (3) In the phase change latent heat stage, the temperature difference (TD) of phase change ventilation device decreases almost linearly over time. (4) The significance analysis of orthogonal experiment shows the impact of various factors on the cooling performance of phase change ventilation device as follows: IAV > IAT > PCPT > PCT > TCEM.

Keywords: Phase change plates; Free cooling; Phase change ventilation device; Heat transfer; Data centers

Nomenclature

Greek symbols		Subscripts	
c_p	Specific heat capacity of air, kJ/(kg·K)	T_{pcm}	Temperature of phase change materials, °C
u	Volume flow rate of air, m^3/s	T_s	Solid phase temperature of phase change materials, °C
ρ	Density of air, kg/m^3	T_l	Liquid phase temperature of phase change materials, °C
ν	Dynamic viscosity, $(N \cdot s/m^2)$	Acronyms	
P	Static pressure, (Pa)	PCP	Phase change plates
q_T	Volumetric heat source, (W/m^3)	PCM	Phase change material
K	Thermal conductivity, (W/(m·K))	IAV	Inlet air velocity
T	Temperature, °C	IAT	Inlet air temperature
t	Time, s	PCPT	Phase change plate thickness
λ	Liquid volume fraction	PCT	Phase change temperature
k	Turbulent kinetic energy, (J/kg)	TCEM	Thermal conductivity of encapsulation material
ε	Turbulent energy dissipation, J/(kg·s)	TD	Temperature difference

1 Introduction

As a large-capacity place, the increasing number and scale of data centers have led to rapid growth in energy consumption [1, 2]. In 2018, Chinese data centers consumed a total of 15 billion kWh of energy, accounting for 2.19% of social energy consumption [3]. In 2023, Chinese data centers consumed a total of 266.7 billion kWh of energy, accounting for 2.89% of social energy consumption. From 2016 to 2030, global data center's power demand is expected to rise from 286 TWh to approximately 321 TWh [4] . Traditional data centers rely primarily on mechanical cooling from air conditioning systems, and its air conditioning energy consumption accounts for about 40% of the total energy consumption of the data center [5, 6]. The increase in data center energy consumption is inevitable, therefore, using cooling energy saving strategies to reduce data center energy consumption is the current challenge [7]. Free cooling and thermal energy storage are two energy-saving strategies for reducing data center energy consumption. [8, 9]. Free cooling is a method that utilizes natural cold sources, widely employed in large data centers with temperate climates[10]. It is divided into air side free cooling, water side free cooling and heat pipe free cooling [11-13]. Thermal energy storage is one such technology that helps reduce peak loads in data centers and enhances energy efficiency [14]. It can overcome mismatches in energy supply and demand across time, temperature, and location [15]. However, both cooling strategies have their own drawbacks.

In regions with mild climate and large temperature difference (TD) between day and night, the air-side free cooling method has good energy-saving potential [16, 17]. Luis Silva-Llanca et al. [13] studied the energy-saving effects of natural air-side cooling under various weather conditions. The results showed that the effects are more favorable in locations with lower temperatures and higher humidity. Lan J et al. [18] numerically simulated the energy-saving potential of the combination of air side natural cooling and fan wall in Guizhou, a region with mild climate. The results showed that, according to the developed model, the fan wall natural cooling technology can save approximately 34% in energy consumption. Zhang et al. [19] analyzed and compared the main characteristics and energy-saving effects of several typical free cooling strategies. The results showed that direct fresh air cooling has the highest potential for free cooling. Oro E et al. [20] assessed the feasibility of using a 1250 kW direct air-side cooling system in data centers across various regions. The results showed that this system can lower energy consumption by approximately 15-22%. Endo et al. [21]

investigated the use of direct air-side cooling to reduce energy consumption in data centers. The study showed that this cooling method saves 20.8% of energy per year compared to a data center using conventional air conditioning. However, the intermittency of natural cold source is a difficult problem to be considered in its practical application, and thermal energy storage can solve this problem.

Thermal energy storage can store unstable energy and release stable energy when needed [22, 23]. Therefore, thermal energy storage can enhance the efficiency of natural cold sources and the flexibility of cooling systems. Phase change materials (PCMs) with high energy density are a common thermal energy storage medium [24, 25]. It is capable of storing a vast amount of energy within a narrow temperature range, effectively addressing the discrepancy between energy supply and demand [26, 27]. The technology of energy storage through phase change is extensively employed in the domain of building energy preservation [28-30], solar energy systems [31, 32], air conditioning systems [33, 34] and it is mostly used as an emergency cooling unit in data centers. Huang B et al. [35] designed a phase change energy storage system to provide emergency cooling for modular data centers, with the aim of reducing dependence on uninterruptible power supplies. Experimental results showed that when the IAV is 1.5 m/s, the cooling device can meet the emergency cooling demand for a minimum of 300 seconds. Gholampour M et al. [36] experimentally studied the method of using PCM to extend the duration of emergency cooling in air-cooled data centers. The results showed that the emergency cooling time was extended by about 7 minutes when PCM was used. Ma X et al. [37] proposed a novel cooling system integrating a loop thermosiphon with PCM, and conducted experimental and numerically analyzed on the thermal performance of the system. The results indicated that once the thermal conductivity of PCM reached 2 W/(m·°C), its cooling capacity could meet the urgent cooling requirement within 15 min. Zheng et al. [38] studied an air phase change cold storage system for emergency cooling in internet data centers. The results indicated that the four-level staggered system can provide sufficient cooling capacity for typical cabinets in internet data centers during power emergencies. Therefore, the energy storage characteristics of PCM can fully solve the intermittency challenge of natural cold sources.

In summary, the application of PCM combination with natural cooling sources has a great potential for energy savings in regions with mild climates. According to previous studies, the method of combining PCM with natural cold sources has been applied to thermal management in different scenarios [39-41], but there are still some gaps in the field of data center temperature control that need to be further explored. Furthermore, the technology of phase change energy storage is progressively maturing in the application of data centers. However, its application in data centers is primarily limited to emergency cooling due to the lack of utilization of natural cold sources, making it unable to achieve cyclic refrigeration. Therefore, phase change assisted direct ventilation technology is a compelling topic for research in the temperature control field of data centers. As shown in Fig. 1, the phase change plates (PCPs) solidifies by storing the cold energy in the natural cold air at night. During the day, fresh external air passes through the system's filtering section, phase change cooling section, and air supply section in sequence, then enters the closed hot aisle data room to cool the cabinets, and finally exhausts from the hot aisle. Compared to traditional data center mechanical cooling, this technology achieves a more reliable, flexible, and energy-efficient cooling solution inside data center.

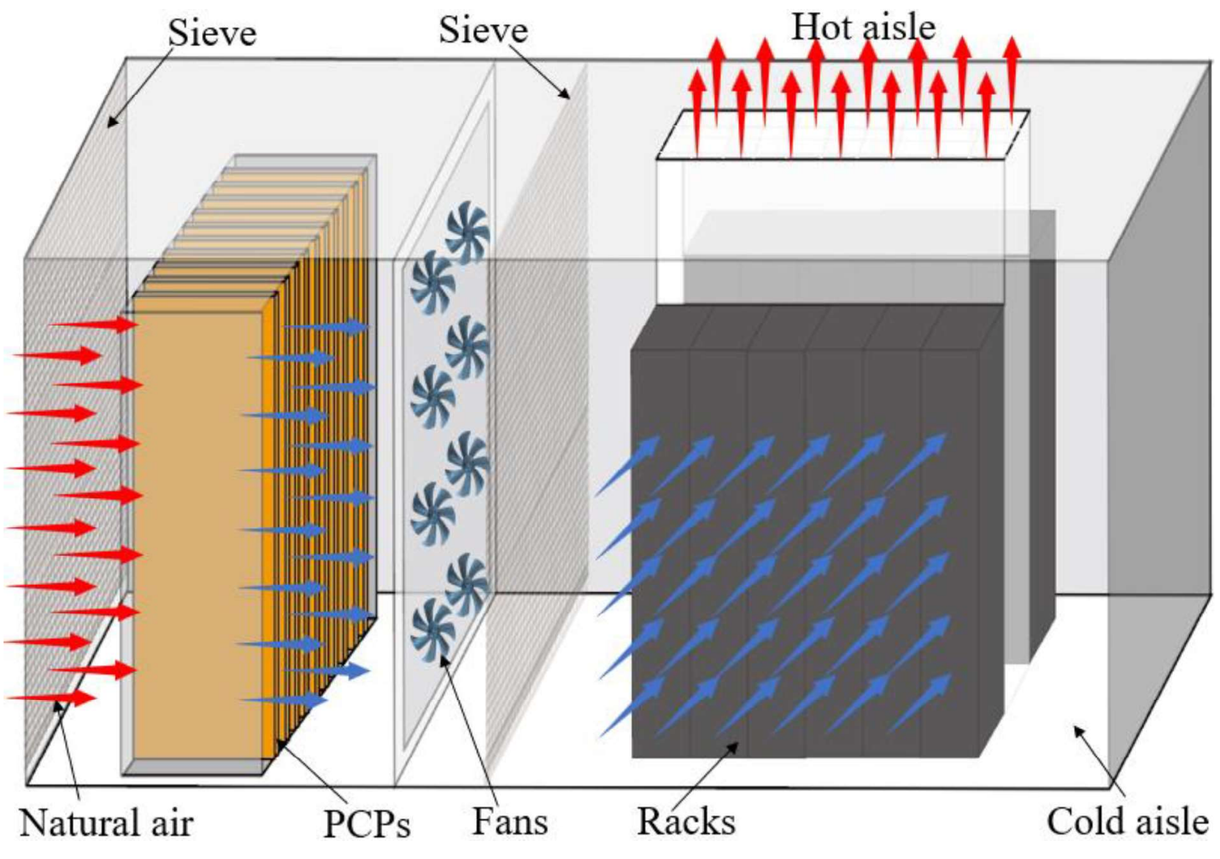

Fig. 1. Phase change assisted direct ventilation schematic diagram.

To address the significant energy consumption in data centers and tackle the sustainability of natural cooling, this paper proposes and numerically simulates an advanced cooling system that leverages phase change-assisted direct ventilation technology. Through experimental research, the feasibility of this model is verified, and its cooling performance is evaluated via numerical simulation.

Additionally, the study employs orthogonal experiments to investigate the impact order of five key factors—namely, inlet air velocity (IAV), inlet air temperature (IAT), phase change plate thickness (PCPT), phase change temperature (PCT), and thermal conductivity of the encapsulation material (TCEM) on the cooling performance of the phase change ventilation device. The results elucidate the influence laws and degrees of these factors on the device. This research provides valuable guidance for the continuous natural cooling of phase change ventilation devices in data centers.

2 Methodology

2.1 Experimental details

2.1.1 Experimental equipment and principle

The experimental platform of this study is shown in Fig. 2 (a), which is connected by the laboratory of Guizhou University and a phase change ventilation device. The laboratory is equipped with a ventilation room and a cooling room, which are connected by a window. The ventilation room is connected to a thermostat control system to control air temperature. In Fig. 2 (b), the dimensions of acrylic transparent channel (5 mm thick) are 2 m (L)×0.65 m (W)×0.65 m (H). In Fig. 2 (c), each PCP measures 1.15m (L) × 0.59m (W) × 0.03m (H), with packaging material make of 1 mm thick galvanized sheet and fill with PCMs. Paraffin wax serves as a typical organic PCM, featuring its advantages including no pollution, non-corrosion, low cost, high heat storage capacity and relatively stable performance, which makes it have certain competitiveness in practical application[42, 43]. ASHRAE recommends a maximum supply air temperature of 27°C for data centers. Therefore, this article uses paraffin with a PCT below 27°C. Table 1 displays the thermal performance characteristics of paraffin wax. Fig. 3 displays the photos of the experimental equipment, while Table 2 presents the precise parameters.

(a) Experimental platform

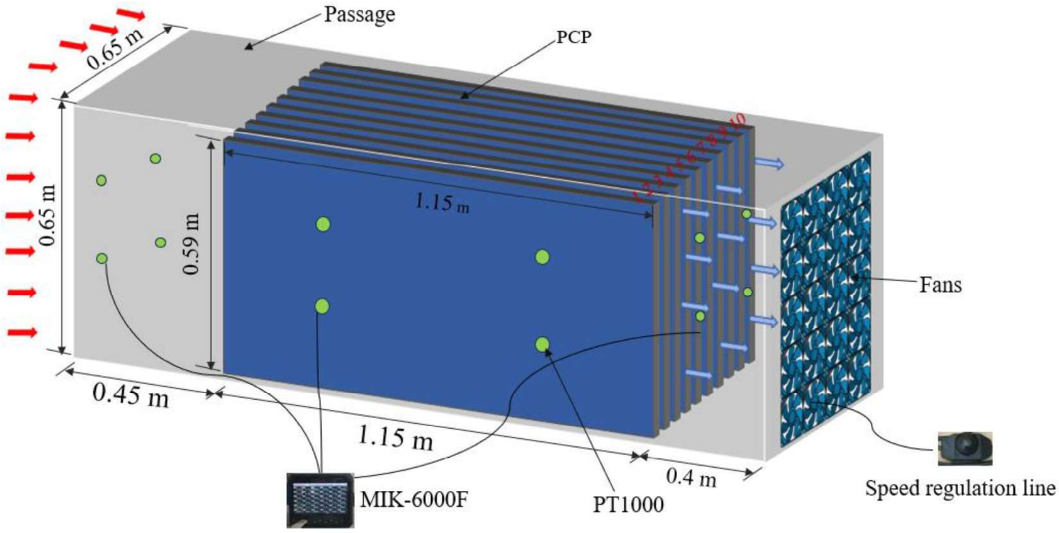

(b) Phase change ventilation device

(c) Phase change plate diagram

Fig. 2. Experimental platform and device.

(a) Data collection **(b) Thermal resistance** **(c) Anemometer** **(d) Fan**

Fig. 3. Diagram of experimental equipment.

Table 1. The thermal performance characteristics of paraffin.

Material	paraffin
Phase change temperature (°C)	25.84
Density (kg/m^3)	880
Thermal conductivity(W/(m·K))	0.21
Latent heat (kJ/kg)	165.9
Specific heat (kJ/(kg·K))	3.22

Table 2. Main design parameters of equipment.

Equipment name	Equipment type	Accuracy	Range	Remark
Data collection	MIK-6000F	Read value × 0.5% + 1 °C	-200 ~ 800°C	Work environment: 20 ~ 90%
Thermal resistance	PT1000	± 0.01°C	-50 ~ 200°C	Length of the line: 4 m
Impeller-type anemometer	FLUKE-925	Full scale ± 2%	0.40 ~ 5.00 m/s	Work environment: 0 ~ 50 °C
Fan	SF8025AT	± 0.05 m^3/min	2 m^3/min	Dimension: 12 cm × 12 cm

Fig. 4 presents the experimental schematic diagram. During the cooling release phase of PCPs, outdoor fresh air is drawn into the ventilation pipeline by an exhaust fan. Within the pipeline, the fresh air is conditioned to the required temperature through the heating and spray sections of the thermostat control system before being blown into the ventilation room by a fan. To minimize heat loss, the connecting window between the ventilation room and the cooling room is closed during this process. Subsequently, the conditioned hot air is directed into the phase change ventilation device for cooling treatment, facilitated by 20 small fans whose speed is controlled by a speed regulation line. During the cooling phase of the PCPs, the cold air fan is activated. The outdoor fresh air is cooled by the evaporator of the cold air fan, simulating nighttime cooling conditions. This cooled air is then recirculated within the cooling room. To maintain the cold air environment, the connecting window is opened, and the hot air intake is closed to prevent air inflow and cold loss. The cooled air is then directed into the ventilation device, where it solidifies the PCPs under the action of the fans, completing the cooling.

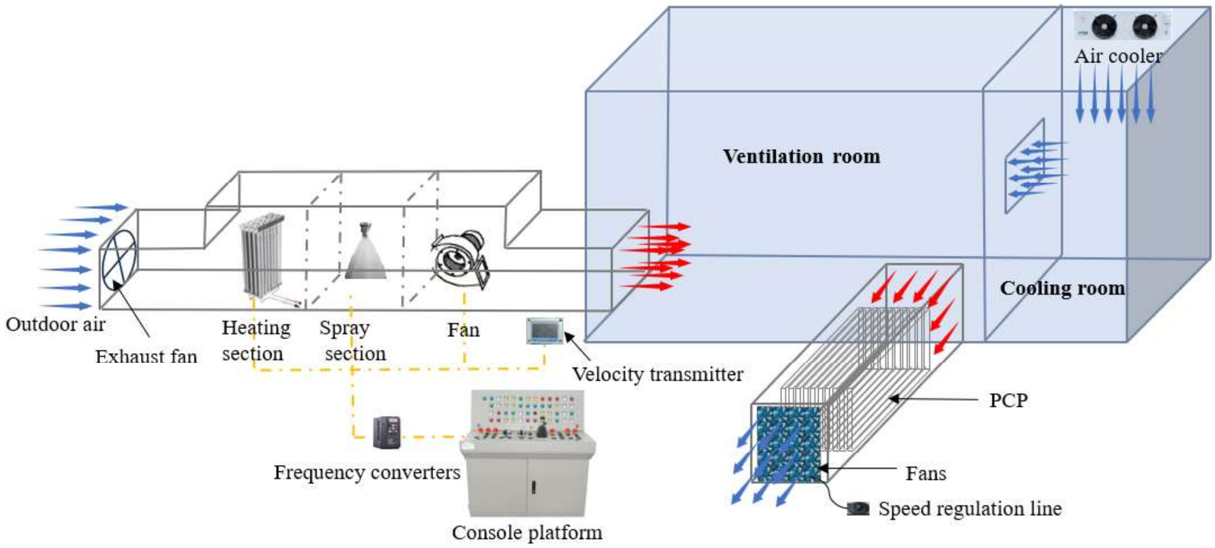

Fig. 4. Experimental schematic diagram.

2.1.2 Data collection

The TD that can be handled by ventilation device is a crucial indicator for assessing its cooling performance. In Fig. 5 (a), the measuring points are located 5cm from the inlet and 20cm from the outlet. Fig. 5 (b) illustrates the distribution of 4 inlet measurement points and 4 outlet measurement points. Four measuring points are positioned in the central plane of each PCP, as shown in Fig. 5 (c). Temperature measurements are taken by PT1000, with data recorded and saved by MIK-6000F.

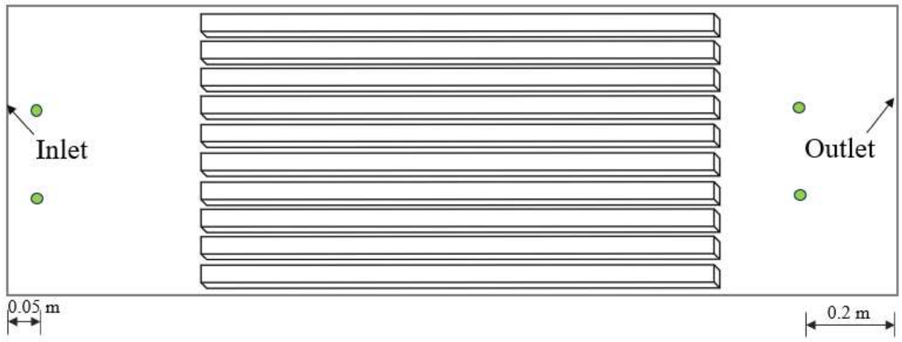

(a) The position of the measuring points relative to the inlet and outlet

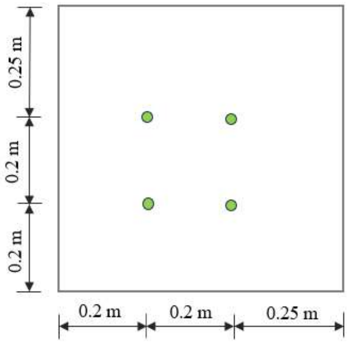

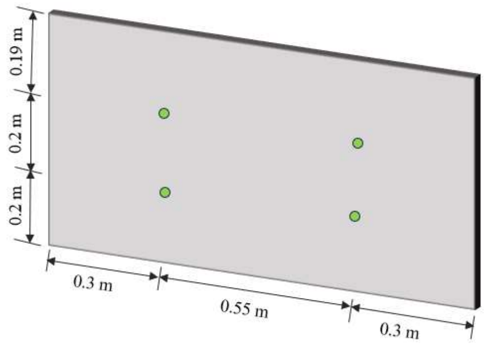

(b) Inlet and outlet measurement points **(c) Measurement points in the PCP**

Fig. 5. Temperature measurement points of phase change ventilation device.

2.1.3 Experimental cases

This experiment primarily studied the impact of IAV on the cooling efficiency of a phase change ventilation devices. The case design is presented in Table 3. The IAT is 32°C, the IAV are 1.5 m/s and 2 m/s, the number of PCP is 10, and the PCPT is 3 cm.

Table 3. Experimental Cases.

Case	IAV (m/s)	IAT (°C)	Number of PCPs	PCPT (cm)
1	1.5	32	10	3
2	2	32	10	3

2.1.4 Experimental procedures

Taking case 1 as an example, with an IAV of 1.5 m/s, an IAT of 32°C, 10 PCPs, and PCPT of 3 cm. The following is the main experimental process:

(1) Set up temperature measurement points and fix 10 completely solidified PCPs evenly inside the transparent channel;

(2) Connect the temperature measuring point to the paperless recorder, and configure the storage time of the recorder to 1 min;

(3) Open the thermostat control system to stabilize the average temperature of the inlet measuring point at 32 ± 0.5°C;

(4) Open the fan to control the IAV at 1.5 ± 0.3 m/s and close the connection window;

(5) Stop operation after 8 hours of thermostat control system;

(6) Open the connection window, activate the air cooler, and keep fans running to facilitate the solidification of PCM inside the transparent device;

(7) Repeat the aforementioned experimental steps, changing the operating parameters with case 2;

(8) Organize the temperature data.

2.1.5 Uncertainty analysis

The total uncertainty K of the experiment is calculated by the uncertainty γ and the uncertainty δ, where γ is calculated by the Bessel formula and δ is expressed by the instrument error [44]:

$$\gamma = \frac{s_x}{n} \tag{1}$$

$$s_x = \sqrt{\frac{\sum_{i=1}^{n}(x_i - \bar{x})^2}{n-1}} \tag{2}$$

$$\delta = \Delta_{instrument} \tag{3}$$

$$K = \sqrt{\gamma^2 + \delta^2} \tag{4}$$

Where, x_i is the value of the measurement parameter, and $\bar{x}$ is the arithmetic average. The uncertainty results are shown in Table 4.

Table 4. Uncertainty results.

Item	Units	Accuracy
Measured parameters		
Measuring point temperature	℃	± 0.01
Inlet air velocity	/	± 2%
Calculate parameter		**Uncertainty**
Temperature difference	℃	± 0.035

2.2 Model construction and meshing

This study established a computational model using ANSYS ICEM based on the geometric space of the experiment to investigate the temperature control capability of the ventilation device. In the current model, the dimensions are consistent with the experimental setup dimensions. Using structured grid division, the numerical model has two computational domains, namely the air domain and the PCM domain, as depicted in Fig. 6. To guarantee calculation accuracy, the number of grids on the coupled wall surface has been increased. The interface between the PCP surface and the PCM is a coupled interface. To minimize numerical errors caused by grid size, five different grids (310,800、704,060、924,000、1,221,120 and 1,744,320) are selected for the study of grid independence. In the current simulation work, numerical results with an IAT of 32°C, IAV of 2 m/s, 10 PCPs with a thickness of 3 mm are selected for comparison. Fig. 7 shows the temperature variations at the same point within the PCP and at the outlet of the ventilation device at different time points for different grid numbers. When the grid is less than 924,000, both the measuring point temperature and the outlet temperature will change. After that, the number of grids has negligible impact on temperature values. Thus, to enhance accuracy and reduce computational time, a grid model comprising 924,000 grid cells is chosen for analysis.

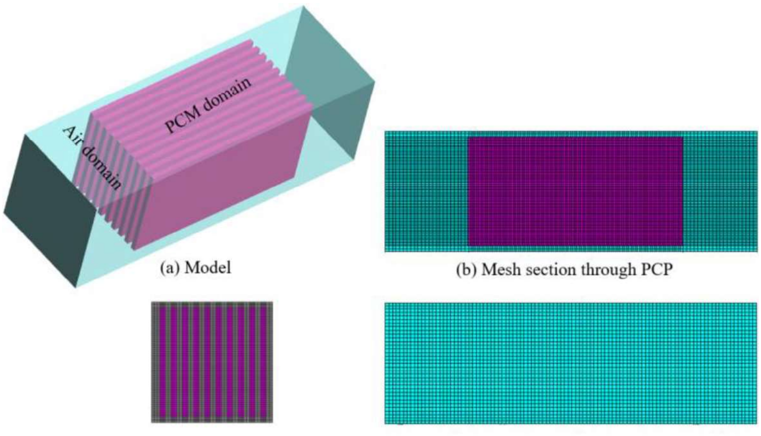

Fig. 6. Numerical model meshing diagram.

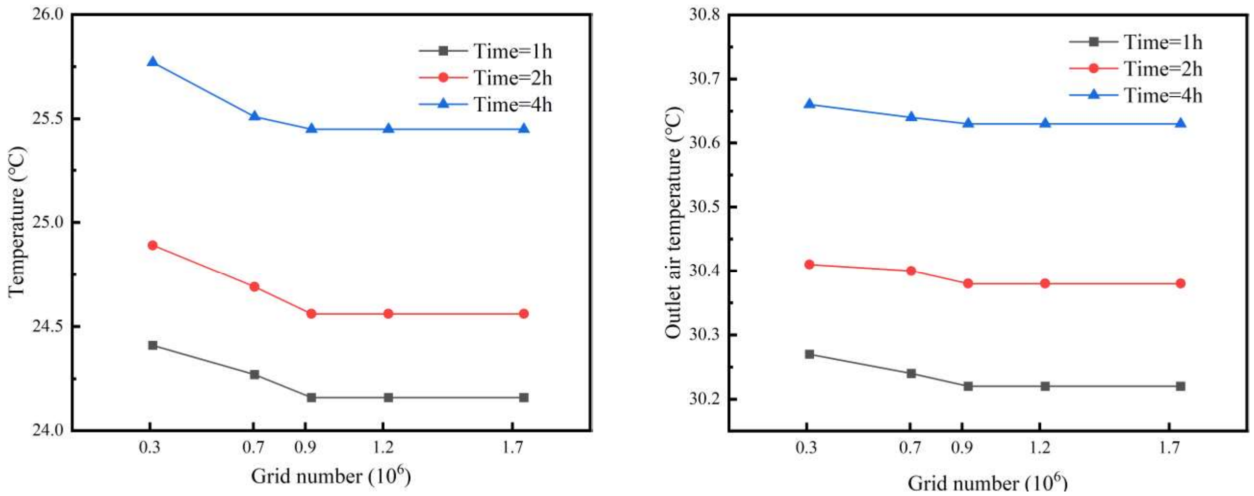

(a) Temperature changes at monitoring point **(b) Temperature change at outlet of ventilation device**

Fig. 7. Temperature changes at 1 h, 2 h, and 4 h of heat exchange under different grid numbers.

2.3 Turbulence model

To ensure high stability and computational accuracy of the model, this paper employs the standard k-ε turbulence model. In addition, thermal conduction in ventilation systems is simulated using a solidification and melting model as well as standard wall surface functions. To streamline the model, the simulation is based on the following assumptions:

(1) The heat source is constant;

(2) The flow of air and PCM is incompressible;

(3) The air flowing in the phase change ventilation device is dry air;

(4) Ignore the volume expansion of PCMs during the melting process;

(5) Assuming the PCM is isotropic, the physical parameters of air and PCM do not change with temperature;

(6) The effect of buoyancy is negligible.

The continuity equation is expressed as[45]:

$$\nabla \cdot u = 0 \tag{5}$$

The momentum equation is expressed as[46]:

$$\rho_{PCM} \frac{\partial u}{\partial t} + \rho_{PCM} \nabla(uu) = -\nabla \mathrm{P} + \nu \nabla^2 u - \frac{(1-\lambda)^2}{(\lambda^3 + \varphi)} A_m u \tag{6}$$

Where u is the velocity vector (m/s); ρ is the material density (kg/m^3); t is time (s); P is static pressure (Pa); ν is dynamic viscosity (N·s/m^2); A_m is paste region constant, whose range is 10^4–10^7, and its value is set to 1×10^5 in the present work; λ is the liquid part of the PCM; φ is a decimal number, set to 0.001 to avoid being divided by zero.

The value of λ is determined by the following formula[46]:

$$\lambda = \begin{cases} 0 & T_{PCM} \le T_s \\ \dfrac{T_{PCM} - T_s}{T_l - T_s} & T_s < T_{PCM} < T_l \\ 1 & T_{PCM} \ge T_l \end{cases} \tag{7}$$

In the above formula, T_{PCM} represents the temperature of PCM; T_s indicates the solid phase temperature of PCM; T_l indicates the liquid phase temperature of PCM.

The energy equation is expressed as[18]:

$$\rho c_p \left(\frac{\partial T}{\partial t} + u \cdot \nabla \mathrm{T} \right) = K \nabla^2 T + q_T \tag{8}$$

Where c_p is specific heat kJ/(kg·K); k is thermal conductivity (W/(m·K)); q_T is volumetric heat source (W/m^3).

The κ and ε transport equations are expressed as[47]:

$$\frac{\partial}{\partial t}(\rho\kappa)+\frac{\partial}{\partial X_i}(\rho\kappa u_i)=\frac{\partial}{\partial X_j}\left[\left(\nu+\frac{\nu_t}{\sigma_k}\right)\frac{\partial k}{\partial X_j}\right]+G_k+G_b-\rho\varepsilon-Y_M+S_k \tag{9}$$

$$\frac{\partial}{\partial t}(\rho\varepsilon)+\frac{\partial}{\partial X_i}(\rho\varepsilon u_i)=\frac{\partial}{\partial X_j}\left[\left(\nu+\frac{\nu_t}{\sigma_\varepsilon}\right)\frac{\partial \varepsilon}{\partial X_j}\right]+C_{1\varepsilon}\frac{\varepsilon}{k}(G_k+C_{3\varepsilon}G_b)-C_{2\varepsilon}\rho\frac{\varepsilon^2}{k}+S_\varepsilon \tag{10}$$

Among them, G_k is the turbulent kinetic energy term; G_b is the turbulent kinetic energy generated by buoyancy; Y_M is the fluctuation generated by the transition diffusion in compressible turbulent flow; ν_t is the turbulent viscosity coefficient; $C_{1\varepsilon}$、$C_{2\varepsilon}$、$C_{3\varepsilon}$ are constants; S_k and S_ε are user-defined source terms.

2.4 Numerical cases

In this paper, the effects of IAV, IAT, PCPT, PCT and TCEM on the cooling performance of phase change ventilation device are studied by orthogonal experiment. In data centers, a IAV range of 1 ~ 4 m/s is one of the common scenarios, which is often considered as a suitable range that can meet the cooling requirements while ensuring uniform airflow. Therefore, the IAV designs in this article are 1 m/s, 2 m/s, 3 m/s, and 4 m/s. ASHRAE recommends a maximum supply air temperature of 27°C for data centers, and based on the highest daytime temperature of 34°C in Guizhou in summer [18], this article selects PCT as 23°C, 24°C, 25°C, 26°C, and IAT as 28°C, 30°C, 32°C, 34°C. The level selection of PCPT is 2 cm, 3 cm, 4 cm, 5 cm. The encapsulation material is stainless steel, with a thermal conductivity ranging from 15 W/(m·K) to 45 W/(m·K), so the thermal conductivity options are 15 W/(m·K), 25 W/(m·K), 35 W/(m·K), and 45 W/(m·K). The numerical cases are shown in Table 5. The thermal properties of the PCM used are shown in Table 6.

Table 5. Numerical cases design.

Cases	IAV (m/s)	IAT (°C)	PCPT (cm)	PCT (°C)	TCEM W/(m·K)
1	1	28	2	23	15
2	1	30	3	24	25
3	1	32	4	25	35
4	1	34	5	26	45
5	2	28	3	25	45
6	2	30	2	26	35
7	2	32	5	23	25
8	2	34	4	24	15
9	3	28	4	26	25
10	3	30	5	25	15
11	3	32	2	24	45
12	3	34	3	23	35
13	4	28	5	24	35
14	4	30	4	23	45
15	4	32	3	26	15
16	4	34	2	25	25

Table 6. Thermal performance of PCM.

Thermo-physical parameters	Value
Density (kg/m^3)	880
Thermal conductivity (W/(m·K))	0.2
Latent heat (kJ/kg)	240
Viscosity (kg/m s)	0.072
Specific heat (J/(kg·K))	2000

2.5 Initial conditions and boundary conditions

The inlet boundary condition of the model is specified as velocity inlet, the values of temperature and velocity are set based on the parameters in Table 5. The outlet is set to be outflow, the interface between the PCP surfaces and the PCM are defined as coupled surfaces, and the other walls are defined as insulation walls. The encapsulation materials of PCPs are all stainless steel, with an initial temperature of 22°C for each operating condition. This simulation uses a pressure-based segregation algorithm, with pressure and velocity coupling implemented using the SIMPLE algorithm. Pressure correction using the PRESTO method. The relaxation factor coefficient remains unchanged at its default value. The convergence criteria for speed, continuity, energy, and dissipation rate remain unchanged, with values of 10^{-3}, 10^{-3}, 10^{-6} and 10^{-3}, respectively.

2.6 Simulation settings

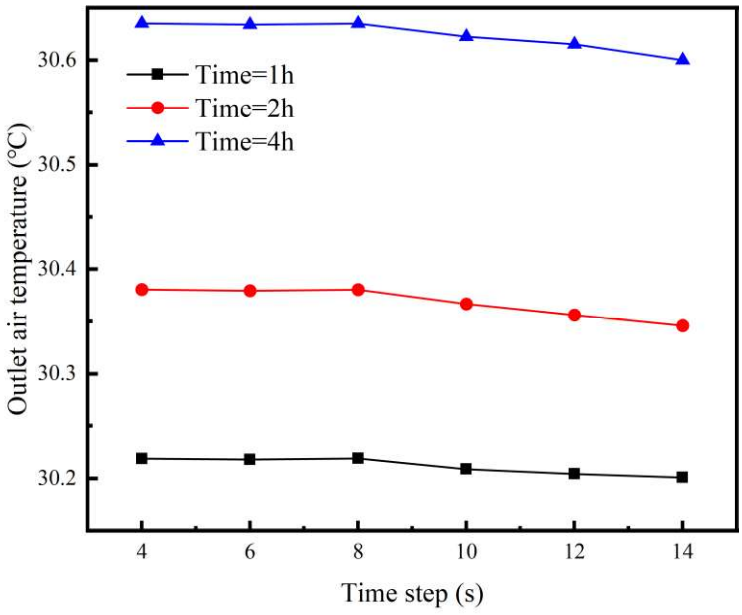

Fig. 8. Time step verification.

Fig. 8 depicts the variation in outlet temperature of the device with time steps after a heat exchange for 1 hour, 2 hours, and 4 hours. The boundary conditions in the numerical calculation process are consistent with the grid independence verification in Section 2.2. In Fig. 8, as the time step exceeds 8 s, the outlet temperature begins to change and increases with the time step. If the time step is shorter than 8 s, the outlet temperature value is almost unchanged. To reduce the computation time, the time step is set to 8 s.

2.7 Model Validation

To validate the model, the numerical results of this work are compared with the experimental research results. The results of experimental cases 1 and 2 validate the reliability of the numerical model. Fig. 9 shows the numerical and experimental TDs and their relative errors of phase change ventilation devices under two different conditions. As shown in Fig. 9, the TD between the inlet and outlet in the experiment and simulation exhibits a similar trend. At the same time point, the relative error ranges from 1.49% to 9.23%. Considering the inevitable measurement errors, the deviation between the experimental value and the numerical value is less than 10%. It indicates that the mathematical heat transfer model established in this study is feasible.

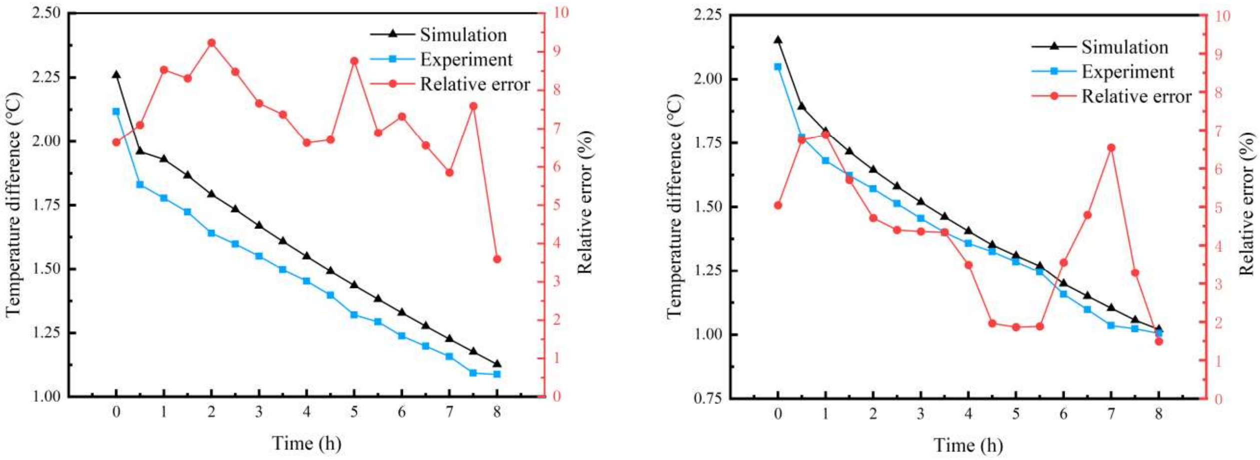

(a) case 1 **(b) case 2**

Fig. 9. Model Validation.

3 Results

3.1 Analysis of cooling performance of phase change ventilation device

In order to analyze the temperature control characteristics of the phase change ventilation device and the heat absorption performance of the PCP more intuitively and clearly, this study selected the case 4 of operating conditions with the most significant effects out of 16 sets for analysis. Under case 4, the IAV is 1 m/s, the IAT is 34°C, the PCPT is 5 cm, the PCT is 26°C, and the TCEM is 45 W/(m·K).

3.1.1 Heat absorption performance of the PCP

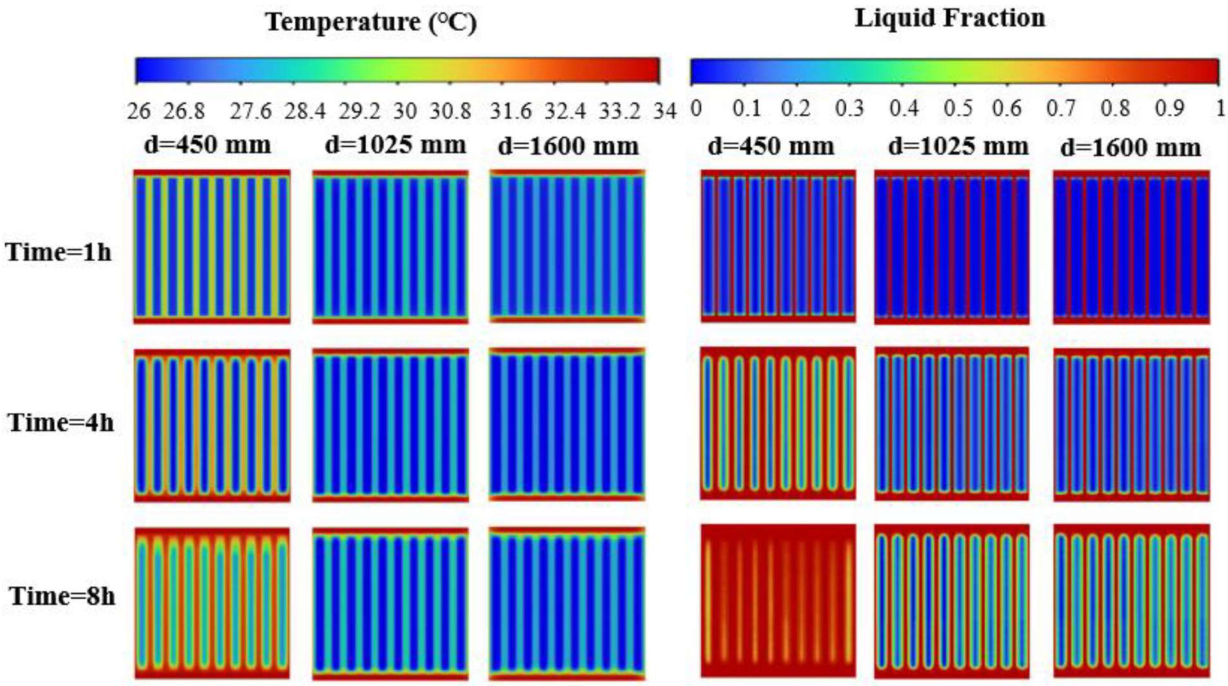

(a) Temperature cloud maps **(b) Liquid phase fraction maps**

Fig. 10. Temperature cloud maps and liquid phase fraction maps of different cross-sections after 1 hour, 4 hours, and 8 hours of heat exchange.

Fig. 10 (a) shows the temperature changes of different sections of the phase change ventilation device at 1 hours, 4 hours and 8 hours. The temperature inside the PCP changes most significantly over time at a distance of 450 mm from the inlet of the device, while the temperature inside the PCP changes less over time at distances of 1025 mm and 1600 mm from the inlet of the device. This indicates that the PCM closer to the device inlet exchanges more heat with the hot air, while the PCM further away exchanges less heat. The temperature of different cross-sections of PCPs also changes at the same time point. The temperature change inside the PCP is most obvious at a distance of 450 mm to 1025 mm from the inlet, and relatively small at a distance of 1025 mm to 1600 mm from the inlet. This indicates that most of the heat transfer process of the PCP is completed in the first half. Fig. 10 (b) shows the variation of liquid fraction of PCPs at different sections after 1 hours, 4 hours, and 8 hours. At the same time point, the melting degree of the front half of the PCP in the figure is higher than that of the back half. This is consistent with the results of Fig. 10 (a), indicating that the heat transfer process of PCP is mostly completed in the front part. At the same time, the liquid fraction of PCP increases with time. In the early stage of melting (1 hours), the liquid fraction of PCP changes slightly, indicating that both sensible heat and latent heat are involved in the heat transfer of the PCP in the first hour. After 8 hours of heat exchange, the liquid fraction of the PCP changes significantly, and the PCM is not completely melted. At this stage, the heat exchange mainly relies on the latent heat of the PCP.

3.1.2 Phase change ventilation device cooling performance

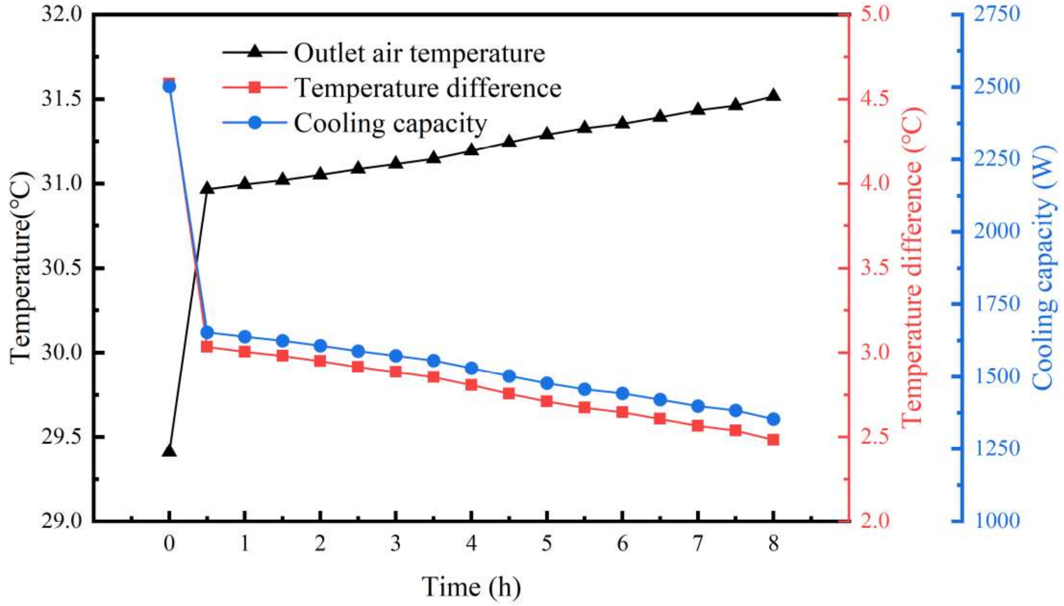

Fig. 11. Changes of outlet temperature, TD and heat flow over time of phase change ventilation device.

Fig. 11 shows the variation of outlet temperature, TD, and heat flow amount of the phase change ventilation device within 8 hours. When the IAT is maintained at 34°C, with the increase of simulation time, the outlet temperature of the ventilation device rises, and the TD decreases. This indicates that the temperature control characteristics of the ventilation device weaken over time. During the initial phase of heat exchange (0.5 hours), the outlet temperature of the ventilation device and the TD change significantly. This is because during this period, most PCMs have not yet started to melt and are still in a solid state, indicating that the sensible heat transfer stage is in progress. From 0.5 hours to 8 hours, the outlet temperature of the ventilation device gradually increases with time. At the same time, the TD decreases gradually and almost linearly with time. This is because during this period the PCM undergoes a phase change and enters the stage of latent heat transfer. As the heat exchange process continues, the degree of phase change of PCM inside the ventilation device increases, leading to a decrease in its temperature control ability. As a result, the TD decreases gradually and the outlet temperature increases slowly. After 8 hours of heat exchange, the TD of the phase change ventilation device decreased from 4.59°C to 2.48°C. The trend of heat exchange is consistent with the trend of TD in the graph. As time goes on, the heat exchange between the PCP and the air decreases, indicating that the cooling capacity of the phase change ventilation device gradually weakens over time. This is due to the decrease in TD for heat transfer. At the same time, the molten PCM also has a certain obstacle to the transfer of heat to the interior, thus affecting the heat exchange capacity. After 8 hours, the heat exchange capacity between PCPs and air decreased from 2501.83 W to 1353.5 W, indicating a decline of approximately 46%, and the average cooling capacity over 8 h is 1571.2W.

The energy consumption formula is:

$$p = \frac{Q}{EER} \tag{11}$$

Among them, Q is cooling capacity; EER is energy efficiency ratio, and Zhou et al. [48] studied that the maximum energy efficiency ratio of a certain data center is 14.5. It is concluded that the device can save a minimum of 108.36W of electricity per hour under working condition 4.

3.2 Sensitivity analysis

3.2.1 Effect of the IAV

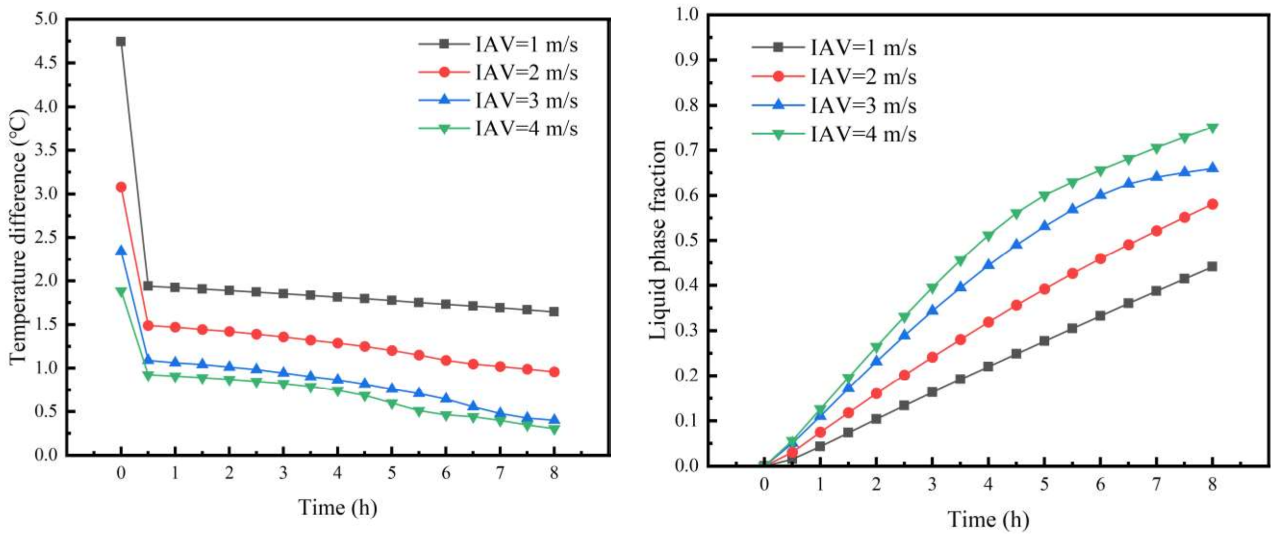

(a) Effect of IAV on TD **(b) Effect of IAV on liquid phase fraction**

Fig. 12. Effect of IAV on cooling performance.

With the test period of 8 hours, keeping the IAT, PCPT, PCT, and TCEM constant, Fig. 12 shows the influence curve of IAV on the cooling performance of the phase change ventilation device. In Fig. 12 (a), the TD decreases with increasing test time across all working conditions. Different inlet air velocities significantly impact the cooling effect of the phase change ventilation device. As IAV increases, the TD treated by the ventilation device decreases, indicating that the cooling performance deteriorates with higher IAV. This is attributed to the faster airflow, which reduces the heat exchange time with the PCPs and leads to insufficient heat transfer between the hot air and the PCM. Consequently, the device outlet temperature rises, and the TD decreases. After 8 hours of simulation with IAV values of 1 m/s, 2 m/s, 3 m/s, and 4 m/s, the TD trends of the ventilation devices are consistent. The TD rapidly decreases within the first 0.5 hours and then gradually declines over time. The TD values after 8 hours of heat exchange for each condition are 1.644°C, 0.958°C, 0.401°C, and 0.304°C, respectively. As IAV increased from 1 m/s to 4 m/s, the average TD of the phase change ventilation device decreased by 1.241°C, and the average cooling efficiency decreased by 62.93%. This demonstrates that IAV has a substantial impact on the cooling performance of the phase change ventilation device. In Fig. 12 (b), the liquid phase fraction of each operating condition increases with the increase of IAV. This is because as the IAV increases, according to the heat transfer formula, the heat transfer between the PCM and the air also increases, so the melting degree of the PCP also increases. After 8 hours heat transfer, the liquid phase fraction of each condition is 0.441, 0.581, 0.660 and 0.752, respectively. In summary, excessive IAV compromises the cooling efficiency of phase change ventilation device, but also shorten the melting time of PCMs, which is detrimental to the sustainable temperature control of PCMs.

3.2.2 Effect of the IAT

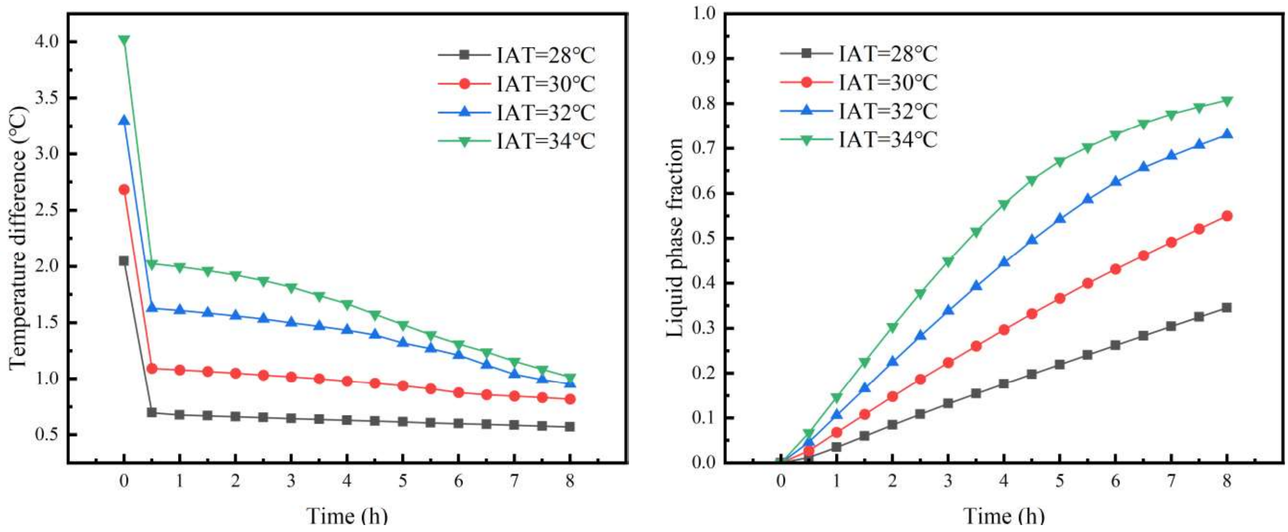

(a) Effect of IAT on TD **(b) Effect of IAT on liquid phase fraction**

Fig. 13. Effect of IAT on cooling performance.

With the test period of 8 hours, and the influence curve of IAT on the cooling performance of the phase change ventilation device is drawn in Fig. 13 when the IAV, the PCPT, the PCT and the TCEM are unchanged. In Fig. 13 (a), the TD of each operating condition decreases with time, and different IATs have a significant impact on the cooling effect of the phase change ventilation device. The TD of the ventilation device increases with the increase of the IAT, indicating that the cooling effect of the phase change ventilation device is better when the IAT is higher. This is because as the IAT increases, the TD between the air and the PCM increases, and the heat transfer also increases, resulting in a decrease in the outlet air temperature of the device and an increase in the TD. When the IAT is 28°C, 30°C, 32°C, and 34°C, after 8 hours of heat exchange, the TD trends of the ventilation device are basically the same. The TD rapidly decreases within 0.5 hours and then slowly decreases over time. The TDs of each operating condition after 8 hours of heat exchange are 0.571°C, 0.818°C, 0.953°C, and 1.015°C respectively. The liquid phase fraction of each operating condition in Fig. 13 (b) increases with the increase of the IAT. After 8 hours heat transfer, the liquid phase fractions are 0.345, 0.55, 0.73, and 0.808 for different operating conditions. It indicates that the higher the IAT, the more fully PCMs are utilized. In conclusion, the higher the IAT, the more favorable for the cooling performance and material utilization of the phase change ventilation device.

3.2.3 Effect of the PCPT

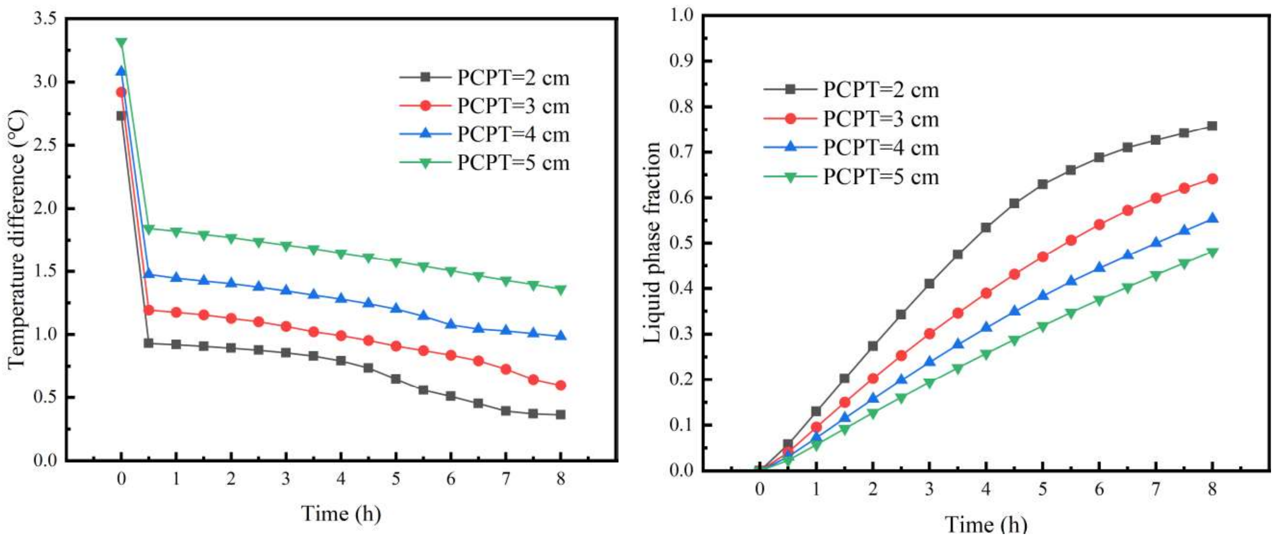

(a) Effect of PCPT on TD **(b) Effect of PCPT on liquid phase fraction**

Fig. 14. Effect of PCPT on cooling performance.

With the test period of 8 hours, and keeping the IAV, IAT, PCT, and TCEM constant, Fig. 14 shows the effect curve of PCPT on the cooling performance of the phase change ventilation device. In Fig. 14 (a), the TD in each working condition decreases with the increase of the test time, and increases with the increase of PCPT, indicating that the thicker the PCP, the better the cooling effect of the phase change ventilation device. With the increase of PCPT, the PCM and its heat exchange area also increase, resulting in an increase in the cold storage capacity and heat exchange rate of the PCP, leading to a decrease in the outlet temperature of the device and an increase in the TD. Moreover, in a channel with a constant width and a fixed number of PCPs, the ventilation duct between the PCPs narrows as the number of PCPTs rises. This causes a minor increase in air flow rate between the ventilation ducts, resulting in a reduced heat exchange time. Nevertheless, based on the experimental findings, this impact is insignificant. When the PCPT is 2cm, 3cm, 4cm, and 5cm, the TD of the ventilation device rapidly decreases within 0.5 hours, and then slowly decreases over time. The TDs of each operating condition after 8 hours of heat exchange are 0.363°C, 0.597°C, 0.986°C, and 1.361°C respectively. The liquid phase fraction of each operating condition in Fig. 14 (b) decreases with the increase of PCPT. Because the thicker the PCP, the slower its melting rate, and the melted PCM will also hinder the transfer of heat to the inside of the PCM. After 8 h heat transfer, the liquid phase fraction of each condition is 0.758, 0.641, 0.553 and 0.481, respectively. In general, too thick PCP will cause the waste of PCM, therefore, it is necessary to control the PCPT within a certain range, while enhancing the performance of the phase change ventilation device, enhance the utilization of PCM.

3.2.4 Effect of the PCT

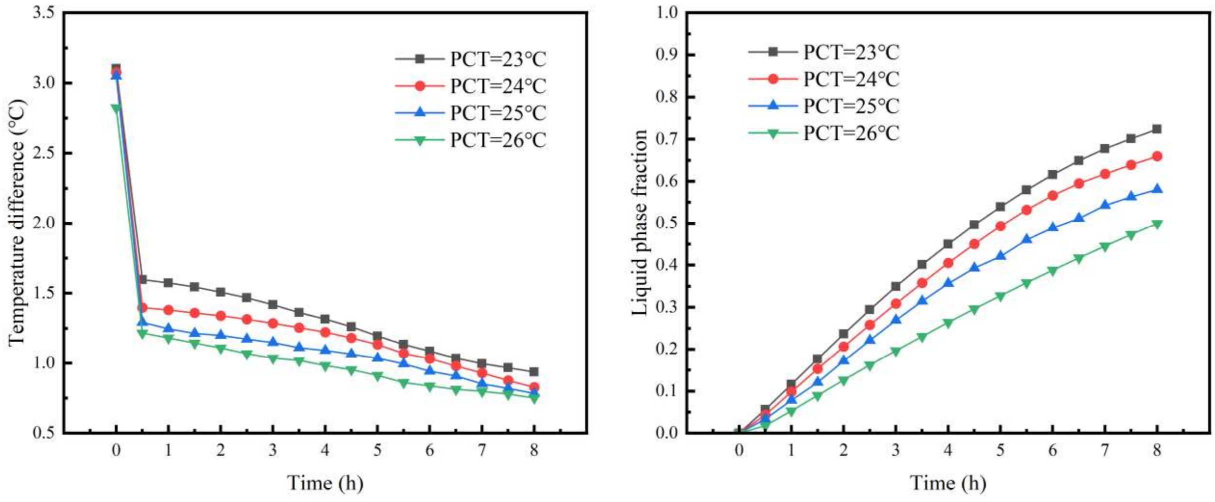

(a) Effect of PCT on TD **(b) Effect of PCT on liquid phase fraction**

Fig. 15. Effect of PCT on cooling performance.

With the test period of 8 hours and keeping the IAV, IAT, PCPT, and TCEM constant, Fig. 15 shows the influence curve of PCT on the cooling performance of the phase change ventilation device. In Fig. 15 (a), the TD decreases with the increase of experimental time under different operating conditions, and the different PCTs of PCMs have a certain influence on the cooling effect of the phase change ventilation device. The TD handled by the phase change ventilation device decreases as the PCT increases, indicating that the cooling efficiency of the device is superior when the PCT is lower. This is because as the PCT decreases, the TD between PCP and air increases, leading to more efficient heat transfer. However, in practical applications in data centers, the PCT should be selected based on the local nighttime average temperature. If the PCT is lower than the local nighttime minimum average temperature, it will result in the PCM not being able to store cold and solidify. In this case, the PCM will completely lose its cooling ability for the data center. Furthermore, a lower PCT will require a longer time for the night solidification PCP, which may result in incomplete solidification within a specified time frame, thereby causing the phase change ventilation device to lose some cooling capacity. After simulating for 8 hours under PCT of 23°C, 24°C, 25°C, and 26°C, the trend of TD changes is basically the same. The TD rapidly decreases within 0.5 hours and then slowly decreases over time. The TDs after 8 hours of heat exchange are 0.935°C, 0.827°C, 0.784°C, and 0.75°C for each operating condition respectively. The liquid phase fraction of each operating condition in Fig. 15 (b) increases with time, with little change in the first 0.5 hours and then gradually becoming more pronounced. Furthermore, the liquid phase fraction decreases with the increase of PCT, this is because a higher PCT leads to a slower melting degree and a smaller proportion of molten PCMs. The liquid phase fractions after 8 hours of heat exchange are 0.724, 0.66, 0.58, and 0.499 for each operating condition respectively. In conclusion, a lower PCT leads to a better cooling performance and material utilization efficiency of the phase change ventilation device.

3.2.5 Effect of the TCEM

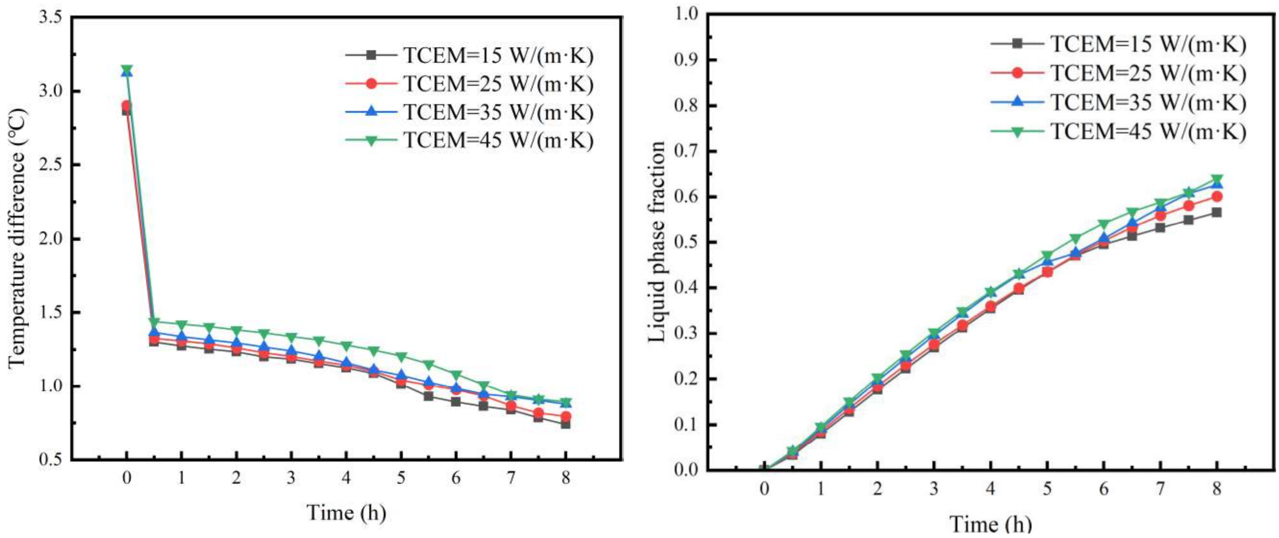

(a) Effect of TCEM on TD **(b) Effect of TCEM on liquid phase fraction**

Fig. 16. Effect of TCEM on cooling performance.

With the test period of 8 hours and constant values for the IAV, IAT, PCPT, and PCT, Fig. 16 shows the effect curve of TCEM on cooling performance of the device. In Fig. 16 (a), the TD under different operating conditions decreases with time and increases with TCEM, indicating that the cooling effect of phase change ventilation device is better when the TCEM is larger. This is because as the TCEM increases, the transfer of heat from the hot air becomes more efficient, resulting in a more efficient heat exchange between the PCM. When the TCEM is 15 W/(m·K), 25 W/(m·K), 35 W/(m·K), and 45 W/(m·K), after 8 hours of heat exchange, the TDs of each condition are 0.74℃, 0.794℃, 0.878℃, and 0.894℃ respectively. The liquid phase fraction of each operating condition in Fig. 16 (b) increases with the increase of the TCEM. The higher the thermal conductivity, the lower the resistance to heat transfer, resulting in a faster melting rate of the PCM. After 8 hours heat transfer, the liquid phase fraction of each condition is 0.566, 0.601, 0.626, 0.64, respectively. In summary, the TCEM has a certain effect on improving the temperature control of the ventilation device.

4 Discussion

4.1 Significance analysis based on orthogonal test

In order to determine the comprehensive influence of five factors, including IAV, IAT, PCPT, PCT, and TCEM on the cooling performance of phase change ventilation device, this study conducted a 5-factor 4-level orthogonal experiment using an $L_{16}(4^5)$ orthogonal experimental table. The average

TD between inlet and outlet of phase change ventilation device within 8 hours is used as the detection index. The energy-saving effect of phase change ventilation device on data centers is better when there is a greater TD. By analyzing the experimental results, key influencing factors can be identified, as shown in the Table 7.

Table 7. Analysis of orthogonal experimental results.

Cases	IAV (m/s)	IAT (°C)	PCPT (cm)	PCT (°C)	TCEM W/(m·K)	Average TD (°C)
1	1	28	2	23	15	0.98
2	1	30	3	24	25	1.46
3	1	32	4	25	35	2.01
4	1	34	5	26	45	2.53
5	2	28	3	25	45	0.55
6	2	38	2	26	35	0.59
7	2	32	5	23	25	2.09
8	2	34	4	24	15	1.83
9	3	28	4	26	25	0.35
10	3	30	5	25	15	0.99
11	3	32	2	24	45	0.92
12	3	34	3	23	35	1.17
13	4	28	5	24	35	0.86
14	4	30	4	23	45	0.95
15	4	32	3	26	15	0.70
16	4	34	2	25	25	0.65
K_1	6.98	2.75	3.15	5.20	4.50	
K_2	5.06	4.00	3.89	5.07	4.55	
K_3	3.44	5.72	5.14	4.20	4.63	
K_4	3.16	6.17	6.46	4.17	4.95	
k_1	1.74	0.69	0.79	1.30	1.13	
k_2	1.27	1.000	0.97	1.27	1.14	
k_3	0.86	1.43	1.28	1.05	1.16	
k_4	0.79	1.54	1.62	1.04	1.24	
Range	0.96	0.85	0.83	0.26	0.11	

As shown in Table 7, the four numbers in row K_i are the sum of the average TDs of inlet and outlet air corresponding to the i level of the five factors. The 4 numbers in the k_i row are the result of dividing the number in K_i by 4. In the same column, the difference between the maximum and minimum values of k_1, k_2, k_3, and k_4 is called the range. A larger range indicates a greater impact of this factor on the experimental indicator. In Table 7, the ranges corresponding to the five factors of IAV, IAT, PCPT, PCT and TCEM are 0.96, 0.85, 0.83, 0.26, and 0.11, respectively. The impact of IAV on the average TD of device is the greatest, followed by the IAT, PCPT, and PCT. The effect of TCEM on average TD of device is the smallest. Further analysis reveals that the k_i corresponding to the 4 levels of IAV are 1.74, 1.27, 0.86, and 0.79, respectively. The value corresponding to the first level is large, that is, the cooling effect of phase change ventilation device is best. In the same way, the optimal level number corresponding to the other four factors can be obtained. Through range analysis, it is concluded that the IAV is the key factor that has the greatest influence on the monitoring index. Based on the numerical case with IAV of 1 m/s, IAT of 34°C, PCPT of 5 cm, PCT of 23°C, and TCEM of 45 W/(m·K), the cooling performance of phase change ventilation device is optimal. In this study, numerical case 4 is similar to the optimal operating condition analyzed, with only one parameter being different. It is the optimal operating case among the 16 operating cases, with an average TD of 2.53°C at the inlet and outlet of the phase change ventilation device after 8 hours of heat exchange. Therefore, numerical case 4 can be considered as the true optimal solution in this study.

4.2 Comparison of several cooling methods

Energy-saving cooling is the current goal of data centers; in order to achieve this goal, predecessors have studied the application of cooling methods such as air cooling, water cooling and natural cooling in data centers. Table 8 compares the six cooling methods in four aspects, emphasizing their respective contributions and challenges. As can be seen from Table 8, although there is currently a cooling method combining PCM and natural ventilation to achieve thermal comfort of buildings, it still deficiencies in the thermal management of data centers. PCM-based cooling is primarily utilized for emergency cooling in data centers and is not capable of providing continuous cooling for data centers. The phase change assisted direct ventilation system currently studied is applied to continuous natural cooling of data centers, filling the shortcoming of PCM combined with natural ventilation applied to data centers. The system combines the advantages of several cooling methods while alleviating their limitations. It brings new opportunities for energy-saving challenges in traditional data center cooling.

Table 8. Analysis of several cooling methods.

Cooling type	Advantages	Major challenges	Application	Duration
Air cooling **[49]**	Easy to implement and maintain, low cost	Low heat dissipation capacity	Data center cooling	Continuous cooling
Water cooling **[50]**	High heat transfer efficiency	High cost, not easy to maintain	Data center cooling	Continuous cooling
Free cooling **[51]**	Utilizing natural cold sources for eco-friendly cooling, saving economic costs	Heavily dependent on geography and climate	Data center cooling	Continuous cooling
PCM-based cooling **[37]**	Implementing emergency cooling for data centers	Difficult to use alone, short cooldown time	Data center cooling	Emergency cooling
PCM combined with natural ventilation **[52]**	Improving the indoor thermal environment of buildings, Save costs	Limited by the natural climate	Thermal comfort of buildings	Continuous
Phase change assisted direct ventilation	Reduce heat transfer steps and energy consumption`	Limited by the natural climate	Data center cooling	Continuous cooling

4.3 Operation strategy of phase change ventilation device

To prevent damage to data centers from dust and high humidity, phase-change direct ventilation systems should be equipped with air filtration and dehumidification systems during their operation. Regions with mild climates, large diurnal temperature variations, moderate relative humidity, and good air quality are more conducive to the operational quality of ventilation devices. A prime example is the Guian region. The operation strategy of the phase change ventilation device in Data Center is depicted in Fig. 17. When the ambient temperature dips below 27°C, cooling devices are not required. At such times, fresh air from the outdoors can be directly channeled into the data center, harnessing natural cooling sources to meet the heat dissipation needs of the server equipment, thereby facilitating energy-efficient operation. In accordance with the ASHRAE cooling guidelines, the recommended temperature range for data centers across all four levels is between 18 and 27°C. When the outdoor fresh air temperature drops below 18°C, the mixed air mode is activated. This entails blending the return hot air from within the data center with the outdoor fresh air, ensuring that the mixed air temperature stays within the recommended range before it is introduced into the data center for server cooling. Should the outdoor ambient temperature exceed 27°C, the fan will direct outdoor fresh air into the phase change ventilation device for cooling treatment, reducing the air temperature entering the data center to below 27°C. If, after cooling, the air temperature still remains above the recommended threshold, additional phase change ventilation devices should be activated to further cool the air. This will bring the temperature down to below 27°C before it is directed to the data center, ensuring that the internal temperature of the data center is always maintained within the appropriate temperature range.

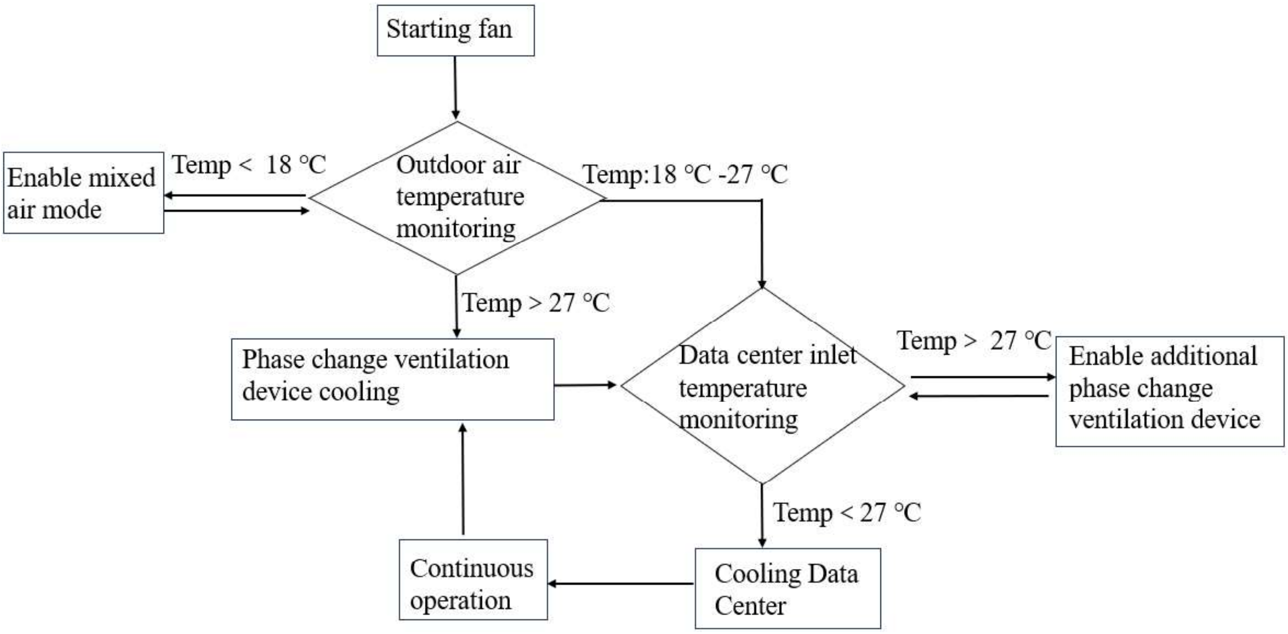

Fig. 17. Operation strategy of phase change ventilation device.

4.4 Future Work

This study primarily investigates the cooling characteristics and influencing factors of the phase change ventilation device. This paper lists 5 influencing factors and designs multiple levels for each influencing factor. Through comprehensive analysis, we have elucidated the laws and degrees of influence these factors exert on the system, thereby providing a robust theoretical foundation for the implementation of phase change-assisted direct ventilation technology. Additionally, the geometric shape, arrangement, and aspect ratio of PCPs significantly impact the temperature control performance of ventilation devices. In current simulations, we observed that the heat exchange process of PCPs is predominantly completed in the first half of their operation. Consequently, in the next phase of research, we will explore the geometry of PCPs, considering designs such as right-angle trapezoids with variable thickness to enhance performance. Secondly, the liquid phase fraction cloud map shows that PCMs cannot completely phase transition in finite time, as the melted PCM hinders the heat exchange of the solidified PCM inside. Therefore, adding fins or perforations to increase the heat exchange area on the basis of the PCP will also be included in the research scope. Finally, the simulations also highlighted limitations in the temperature control capabilities of the ventilation device, particularly in hot weather, where it fails to achieve the maximum recommended inlet temperature for data centers. Drawing on the findings of Gao et al. [53], which demonstrated that PCPs exhibit certain dehumidification functions under specific conditions, we propose incorporating evaporative cooling through sprays in future experiments, in addition to phase change direct ventilation natural cooling. This integration aims to enhance the system's cooling capacity and overall performance.

5 Conclusion

To maximize the utilization of natural cold sources for power conservation and consumption reduction in data centers. In this study, a novel cooling device combining direct ventilation free cooling and PCMs is numerically simulated. The research focuses on the impact of five key factors—IAV, IAT, PCPT, PCT, and TCEM on the cooling performance of the phase change ventilation device. Through orthogonal experiments, the significance of each influencing factor is analyzed in detail. The main conclusions are as follows:

(1) Under Condition 4, the heat exchange between the PCPs and the air decreased from 2501.83 W to 1353.5 W over an 8-hour period, representing a reduction of approximately 46%. The ventilation device is capable of saving 108.36 W of electrical power per hour.

(2) With other factors constant, the average cooling performance of the phase change ventilation device decreases by 62.93% when the IAV increases from 1 m/s to 4 m/s.

(3) During the phase change latent heat stage, the TD of phase change ventilation device decreases almost linearly over time.

(4) The temperature and liquid phase fraction cloud map shows that most of the heat transfer process is completed in the front half of the PCP.

(5) The significance analysis of orthogonal experiment shows the impact of various factors on the cooling performance of phase change ventilation device as follows: IAV > IAT > PCPT > PCT > TCEM.

(6) An operational strategy for the phase change ventilation device under different ambient

temperatures has been proposed.

In conclusion, this article proposes a new method for sustainable natural cooling of data centers. However, humidity is not considered due to limitations in the experimental conditions. Furthermore, this study is currently in the theoretical stage and has not been applied to actual data center racks. When applied in practical engineering, the size of the phase change ventilation device can be determined according to the scale of the data center and local climate data.

Declaration of Competing Interest

The authors declare that they have no known competing financial interests or personal relationships that could have appeared to influence the work reported in this paper.

Acknowledgements

The author would like to thank the financial support the National Natural Science Foundation of China (NO.52168013), the Guizhou Provincial Science and Technology Projects (No. ZK[2022]151).

Data availability

Data will be made available on request.

References:

[1]H. Zhu, D. Zhang, H.H. Goh, S. Wang, T. Ahmad, D. Mao, T. Liu, H. Zhao, T. Wu, Future data center energy-conservation and emission-reduction technologies in the context of smart and low-carbon city construction, Sustainable Cities and Society, 89(2023) 104322.

[2]C. Jin, X. Bai, C. Yang, W. Mao, X. Xu, A review of power consumption models of servers in data centers, APPLIED ENERGY, 265(2020) 114806.

[3]S. Zou, Q. Zhang, C. Yue, S. Du, Effect of servers' arrangement on the performance of a loop thermosyphon system used in data center, APPLIED THERMAL ENGINEERING, 192(2021) 116955.

[4]M. Sermsuk, Y. Sukjai, M. Wiboonrat, K. Kiatkittipong, Feasibility study of a combined system of electricity generation and cooling from liquefied natural gas to reduce the electricity cost of data centres, ENERGY, 254(2022) 124397.

[5]C. Nadjahi, H. Louahlia, S. Lemasson, A review of thermal management and innovative cooling strategies for data center, Sustainable Computing: Informatics and Systems, 19(2018) 14-28.

[6]J. Chu, X. Huang, Research status and development trends of evaporative cooling air-conditioning technology in data centers, Energy and Built Environment, 4(2023) 86-110.

[7]X. Yuan, Y. Wang, J. Liu, X. Xu, X. Yuan, Experimental and numerical study of airflow distribution optimisation in high-density data centre with flexible baffles, BUILDING AND ENVIRONMENT, 140(2018) 128-139.

[8]Q. Zhang, Z. Meng, X. Hong, Y. Zhan, J. Liu, J. Dong, T. Bai, J. Niu, M.J. Deen, A survey on data center cooling systems: Technology, power consumption modeling and control strategy optimization, JOURNAL OF SYSTEMS ARCHITECTURE, 119(2021) 102253.

[9]L. Liu, Q. Zhang, Z.J. Zhai, C. Yue, X. Ma, State-of-the-art on thermal energy storage technologies in data center, ENERGY AND BUILDINGS, 226(2020) 110345.
[10]J. Li, Z. Li, Model-based optimization of free cooling switchover temperature and cooling tower approach temperature for data center cooling system with water-side economizer, ENERGY AND BUILDINGS, 227(2020) 110407.
[11]L. Ling, Q. Zhang, Y. Yu, S. Liao, A state-of-the-art review on the application of heat pipe system in data centers, APPLIED THERMAL ENGINEERING, 199(2021) 117618.
[12]R. Mi, X. Bai, X. Xu, F. Ren, Energy performance evaluation in a data center with water-side free cooling, ENERGY AND BUILDINGS, 295(2023) 113278.
[13]L. Silva-Llanca, C. Ponce, E. Bermúdez, D. Martínez, A.J. Díaz, F. Aguirre, Improving energy and water consumption of a data center via air free-cooling economization: The effect weather on its performance, ENERGY CONVERSION AND MANAGEMENT, 292(2023) 117344.
[14]H. Li, J. Hou, T. Hong, Y. Ding, N. Nord, Energy, economic, and environmental analysis of integration of thermal energy storage into district heating systems using waste heat from data centres, ENERGY, 219(2021) 119582.
[15]H. Mahon, D. O'Connor, D. Friedrich, B. Hughes, A review of thermal energy storage technologies for seasonal loops, ENERGY, 239(2022) 122207.
[16]J. Zhang, R. Mao, C. Li, J. Lan, X. Yi, Z. Zhang, Optimization air-conditioning system and thermal management of data center via fan-wall free cooling technology, APPLIED THERMAL ENGINEERING, 234(2023) 121245.
[17]J. Cho, Y. Kim, Improving energy efficiency of dedicated cooling system and its contribution towards meeting an energy-optimized data center, APPLIED ENERGY, 165(2016) 967-982.
[18]J. Lan, Z. Zhang, X. Liang, H. Wu, G. Wang, R. Mao, Experimental and numerical investigation on thermal performance of data center via fan-wall free cooling technology, APPLIED THERMAL ENGINEERING, 228(2023) 120467.
[19]Y. Zhang, Z. Wei, M. Zhang, Free cooling technologies for data centers: energy saving mechanism and applications, Energy Procedia, 143(2017) 410-415.
[20]E. Oró, V. Depoorter, N. Pflugradt, J. Salom, Overview of direct air free cooling and thermal energy storage potential energy savings in data centres, APPLIED THERMAL ENGINEERING, 85(2015) 100-110.
[21]H. Endo, H. Kodama, H. Fukuda, T. Sugimoto, T. Horie, M. Kondo, Effect of climatic conditions on energy consumption in direct fresh-air container data centers, Sustainable Computing: Informatics and Systems, 6(2015) 17-25.
[22]M. Li, M. Li, X. Xue, D. Li, Optimization and design criterion of the shell-and-tube thermal energy storage with cascaded PCMs under the constraint of outlet threshold temperature, RENEWABLE ENERGY, 181(2022) 1371-1385.
[23]B. Palmer, A. Arshad, Y. Yang, C. Wen, Energy storage performance improvement of phase change materials-based triplex-tube heat exchanger (TTHX) using liquid–solid interface-informed fin configurations, APPLIED ENERGY, 333(2023) 120576.
[24]B. Nie, A. Palacios, B. Zou, J. Liu, T. Zhang, Y. Li, Review on phase change materials for cold thermal energy storage applications, Renewable and Sustainable Energy Reviews, 134(2020) 110340.
[25]B. Peng, M. Qiu, N. Xu, Y. Zhou, W. Sheng, F. Su, Optimum orthogonally structured fins in charging enhancement of phase change materials (PCMs): PCMs' thermophysical properties effects, INTERNATIONAL JOURNAL OF THERMAL SCIENCES, 184(2023) 108005.
[26]K. Du, J. Calautit, Z. Wang, Y. Wu, H. Liu, A review of the applications of phase change materials in cooling, heating and power generation in different temperature ranges, APPLIED ENERGY, 220(2018) 242-273.
[27]M.M. El Idi, M. Karkri, M. Abdou Tankari, A passive thermal management system of Li-ion batteries using PCM